International Journal of Biological Macromolecules 318 (2025) 145302

Contents lists available at ScienceDirect

International Journal of Biological Macromolecules

journal homepage: www.elsevier.com/locate/ijbiomac

A biomimetic reinforced type I/II collagen and hyaluronic acid scaffold in combination with a chondral biomaterial fixation technique for large articular cartilage defect repair: A pilot pre-clinical study

Claudio Intini [a,b,c,d,1], Michael Joyce [a,b,c,1], Michela Uberti [a,b,c], Margot C. Labberté [e], Giulio Brunetti [a,b,c], Becky Hackett [a,b,c], Tom Hodgkinson [a,b,c], John M. O'Byrne [c,f], Pieter A.J. Brama [e], Fergal J. O'Brien [a,b,c,*]

[a] Tissue Engineering Research Group, Department of Anatomy & Regenerative Medicine, Royal College of Surgeons in Ireland (RCSI), Dublin, Ireland
[b] Trinity Centre for Biomedical Engineering, Trinity College Dublin (TCD), Dublin 2, Ireland
[c] Advanced Materials and Bioengineering Research (AMBER) Centre, RCSI & TCD, Ireland
[d] Department of Biomedical Sciences, University of Cagliari, Italy
[e] Translational Research Unit, School of Veterinary Medicine, University College Dublin, Dublin 4, Ireland
[f] Professorial Unit, RCSI at Cappagh National Orthopaedic Hospital, Finglas, Dublin 11, Ireland

ARTICLE INFO

Keywords:
Collagen-based scaffold
Cartilage repair
Preclinical

ABSTRACT

Successfully repairing large articular cartilage defects remain an unmet clinical challenge. Our lab has previously developed a biomimetic mechanically reinforced type I/II collagen-hyaluronic acid (CI/II-HyA) scaffold, which was proven *in vitro* to effectively support a hyaline-like cartilage formation while providing mechanical properties mimicking healthy cartilage. This initial pre-clinical study aimed to elucidate the chondral regenerative capacity of this collagen-based scaffold to repair large clinically challenging articular cartilage defects in goats. Furthermore, a biomaterial-fixation technique - previously tested *ex-vivo* - was also assessed *in vivo*. Scaffolds were implanted into large cartilage defects (8 mm diameter) in a load-bearing area of goat medial femoral condyles and fixed in place using this new fixation technique with either resorbable or non-resorbable sutures. Following 6 months implantation, scaffolds showed promise to repair the large chondral defects. Macroscopic and histological evaluation showed new hyaline-like cartilage formation partially covering the defect area in 3 out of 6 cartilage defects. Moreover, microCT analysis revealed that all scaffolds showed indications of being successfully secured in the defect. Taken together, the biomimetic reinforced CI/II-HyA scaffold in combination with the innovative fixation method provides strong promise to become a viable treatment to currently limited large articular cartilage repair strategies in the clinic.

1. Introduction

When damaged or injured, the cartilage in articular joints experiences a loss of function which can lead to joint degeneration and ultimately development of osteoarthritis (OA) [1–3]. To date, knee OA is the most common type of arthritis and negatively affects an estimated 350 million people worldwide by drastically decreasing the patient's quality of life [4,5]. This prevalence is reflected in the unprecedented and enormous healthcare costs associated with the treatment of OA, which amount to estimated general expenses of around 1–2.5 % of the Gross Domestic Product (GDP) in Western developed economies [5]. Surgical intervention is often necessary for the treatment of severe articular cartilage lesions [6]. Depending on the severity and size of the lesion, a number of conventional surgical options exist, these include bone marrow stimulation (BMS) techniques, chondrogenic cell implantation (autologous chondrocyte implantation), and cartilage graft-based repair (mosaicplasty) and ultimately full knee arthroplasty [6,7]. Although some positive results with small critical sized defects (<6 mm diameter),

* Correspondence to: F.J. O'Brien, Tissue Engineering Research Group, Department of Anatomy & Regenerative Medicine, Royal College of Surgeons in Ireland (RCSI), Dublin, Ireland.
E-mail address: fjobrien@rcsi.ie (F.J. O'Brien).
[1] C. Intini, and M. Joyce contributed equally to this work.

https://doi.org/10.1016/j.ijbiomac.2025.145302
Received 5 March 2025; Received in revised form 28 May 2025; Accepted 14 June 2025
Available online 16 June 2025

outcomes are typically poor for larger lesions (≥8 mm diameter) [8,9]. Consequently, patients are often required to undergo revision surgery, which often results in inferior outcomes on both a short- and long-term basis [6,7]. Thus, a clear clinical need for improved treatments for large articular cartilage injuries capable of fully restoring the long-term functionality of the damaged tissue in patients remains [10].

To this end, tissue engineered cartilage constructs have been developed and have shown some promise as strategies to treat cartilage defects [11,12]. However, successful validation of such constructs in large animal pre-clinical models has proven challenging, thus limiting their translation to the clinic [13–15]. Typically, these new constructs tend to fail, revealing major issues with integration into the native tissue, overall joint inflammation and phenotypic instability of the regenerated tissue [16–19]. Much ongoing research is focused on improving the suitability of advanced constructs to direct successful cartilage repair. For instance, previous studies have shown that appropriate construct architecture, including high porosity and appropriate pore size, is important to facilitate enhanced cellular migration, viability and chondrogenic response [20–23]. These features are crucial for a biomaterial to achieve a high standard of integration and subsequent repair *in vivo*. Furthermore, biomaterials with a high biomimetic nature, resembling native cartilage tissue, show promise in promoting tissue integration and stability, leading to hyaline-like cartilage repair while limiting inflammation and further joint degeneration to post-traumatic OA [24–28]. Typically however, these constructs are only capable of treating small joint defects.

Building on this knowledge, highly porous biomimetic collagen-based scaffolds for cartilage repair have been successfully developed in our laboratory and have demonstrated to support hyaline-like cartilage formation when tested *in vitro* and *in vivo* preclinical models [25,29,30]. In particular, a type I/II collagen and hyaluronic acid (CI/II-HyA) scaffold has demonstrated promise in increasing stable chondrogenic differentiation of mesenchymal stem cells (MSC) with a reduced risk of hypertrophic chondrocyte formation [31–33]. When this scaffold was integrated into a multi-layered scaffold developed specifically for small (<6 mm diameter) critically-sized osteochondral defects, it demonstrated a significant capacity to heal cartilage in small osteochondral defects in rabbit, goat and horse models [29,30,34]. However, to enhance its potential to restore much larger chondral defects (≥8 mm of diameter), we introduced a mechanical 3D printed polycaprolactone (PCL) reinforcement to improve the mechanical properties while retaining the pro-chondrogenic ones [35,36]. *In vitro* assessment proved for this biomimetic reinforced CI/II-HyA scaffold to possess an increased compressive modulus (0.67 MPa) mimicking the physiological range of healthy cartilage (0.5–2.0 MPa) while sustaining improved production and greater spatial distribution of sulphated glycosaminoglycans (sGAG) throughout the scaffold compared to non-reinforced CI/II-HyA matrices [35,36]. This study aimed to assess the potential of this scaffold to heal large cartilage defects *in vivo*.

Another significant challenge in validating biomaterials for the repair of chondral defects is the lack of effective fixation techniques, capable of securing biomaterial scaffolds to these clinically challenging shallow cartilage defects in the articular joint [15,37]. This significantly limits effective tissue integration and hinders cell-migration and *de-novo* tissue formation in the implanted material [15,37]. Unlike materials developed for osteochondral defects (typically implanted using a press-fit technique into deep defects all the way into the subchondral bone), biomaterials designed for treating the cartilage layer alone typically fail given the anatomical function and biophysical forces exerted on the tissue [14,15,34]. The mechanical properties of the biomaterials, such as stiffness and elasticity, often does not match that of the surrounding native cartilage, thus leading to inadequate load distribution and eventual detachment of the material from the defect [38]. Moreover, cartilage is subject to significant compressive and lateral shear forces that often causes dislodgment of the implanted biomaterials [38]. Therefore, there is a clear clinical need for more effective biomaterial fixation techniques to robustly attach scaffolds in shallow chondral defects. Previous studies investigating the use of sutures to affix biomaterials in chondral defects have failed due the surrounding cartilage tissue, or the biomaterial not having a tensile modulus strong enough resist the suture thread tearing through the material [39–41]. In this context, our laboratory has recently designed a fixation technique capable of securing the previously developed biomimetic reinforced CI/II-HyA scaffold for large chondral defect by anchoring the implant to the subchondral bone using a fixation anchor which is connected to the mechanically reinforced scaffold by a suture thread [35]. Specifically, this surgical technique proved successful at securing the scaffold within an *ex-vivo* cadaveric porcine tibial condyle defect model ensuring effective close contact of the biomaterial's edges to the extremity of the cartilage defects [35]. The present study assessed this cartilage biomaterial fixation technique in an *in vivo* environment.

Furthermore, this study aimed to validate the effectiveness of the proposed chondral biomaterial fixation technique including comparison of two different surgical procedures using resorbable and non-resorbable suture threads respectively. In orthopaedic surgical procedures, non-resorbable sutures are often primarily chosen given the major advantages provided in terms of mechanical stability and support compared to the resorbable ones which offer limited long-term support [42]. On the other hand, resorbable suture are more biocompatible and commonly offer advantages with reduced risk of infections and inferior scarring while having inferior mechanical stability for this type of orthopaedic procedure compared to non-resorbable ones [42]. To the best of our knowledge, no previous studies have reported a surgical procedure comparable to the one proposed in this study for large chondral biomaterial fixation. Therefore, it is essential to assess and validate our primary choice of suture threads for this type of surgical procedure *in vivo*.

Taken together, the main objective was to elucidate the capacity of the biomimetic reinforced CI/II-HyA scaffold to repair large (8 mm diameter) articular cartilage defects in the goat medial femoral condyle - a load bearing area in the goat stifle joint – in a pilot preclinical study. Furthermore, we aimed to validate the effectiveness of the chondral biomaterial fixation technique including comparison of two different approaches using resorbable and non-resorbable suture threads respectively.

2. Materials and methods

2.1. Fabrication of the reinforced collagen-based scaffolds for chondral repair

To fabricate the biomimetic reinforced CI/II-HyA scaffolds with mechanical properties similar to healthy cartilage while maintaining the bioactive biological properties, a 3D printed polycaprolactone (PCL) (37KDa) framework with a specific gyroid design pattern was used and incorporated into a pro-chondrogenic collagen-based matrix as previously described (Fig. 1A) [35]. Briefly, the 3D printed PCL framework was printed with an Allevi II printer (3D Systems), producing a scaffold with a compressive modulus (0.67 MPa). Subsequently, the PCL mesh was surface treated using 2 ml per scaffold of 3 M NaOH, for 48 h without shaking or agitation, to increase hydrophilicity of the polymer and integration of the regenerative matrix. The PCL frameworks were then rinsed three times in distilled de-ionized water and incorporated into a collagen-based slurry consisting of type I/II collagen (CI/II) and hyaluronic acid (HyA). The CI/II-HyA collagen-based slurry was prepared with a total collagen concentration of 0.5%w/v and a hyaluronic acid concentration of 0.05%w/v as previously described [43]. The composite PCL-C/II-HyA scaffolds were freeze-dried (Epsilon 1–4 LSCplus, Martin Christ, Germany) together at a constant cooling rate of 1 °C/min to a final temperature of −20 °C. The reinforced PCL-CI/II-HyA scaffolds, and re-threaded Twinfix-Ti osteo-suture anchors were gas sterilized with ethylene oxide in an AN74i chamber (Anderson

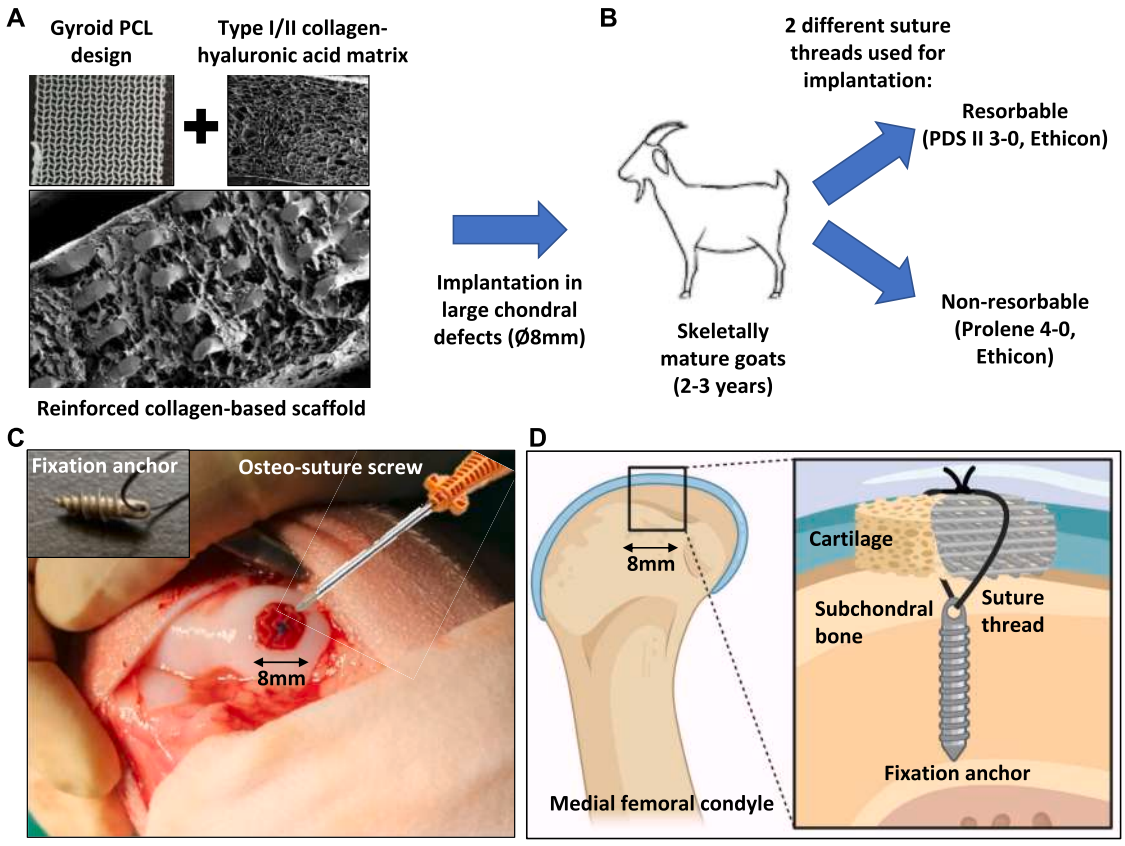

Fig. 1. Illustrative scheme describing the experimental design. (A) Representative SEM images of the biomimetic mechanically reinforced scaffold developed by combining an innovative 3D printed gyroid polycaprolactone (PCL) framework with a pro-chondrogenic biomimetic type I/II collagen-hyaluronic acid (CI/II-HyA) matrix [35]. (B) The scaffolds were implanted in large (Ø8mm) articular cartilage defects in the goat medial femoral condyle using a resorbable (PDS II 3–0, Ethicon) or non-resorbable (Prolene 4-0, Ethicon) suture thread. (C) Macroscopic image of the scaffold implanted in the goat medial femoral condyle. (D) Schematic illustration describing the biomaterial fixation technique to secure the scaffold to the chondral defect. A commercially available osteo-suture screw was used to implant the subchondral fixation anchor which was connected to the scaffold by suture thread [35].

Sterilizers, Haw River, NC USA) for 12 h. The sterile scaffolds were then crosslinked with 1-Ethyl-3-(3-Dimethlamniopropyl)-carbodiimide (EDAC) (6 mM per gram of collagen) and N-Hydroxysuccinimide (NHS) at a ratio (EDAC:NHS) of 5:2 M. The crosslinking agents were suspended in 70 % EtOH and filtered through a 0.22 μm diameter filter before scaffolds were crosslinked for 2 hours [44]. The crosslinked scaffolds were then rinsed and aspirated 3 times with sterile PBS and exposed to UV light for half an hour on each side (top and bottom). The scaffolds were then ready for implantation.

2.2. *In vivo large animal study*

To assess the chondral regenerative ability of the composite biomimetic reinforced scaffolds, an *in vivo* assessment was carried out in a goat medial femoral condyle model under ethical approval (University College Dublin-AREC-P-18–17) and an animal licence granted by the Health Products Regulatory Authority (AE18982/P142) [30]. Cell-free scaffolds were implanted in skeletally mature goats (1 female and 2 males) aged 2–3 years, with defects created in either the left and right stifle joint on high load-bearing areas of medial femoral condyles (size: 8 mm diameter and 1–1.25 mm height). The tissue repair was assessed 6 months post-implantation (Fig. 1B).

2.3. *Surgical procedure and scaffold implantation in caprine cartilage defects*

The surgical procedure was adapted from another recent study in our lab which had focussed on deeper osteochondral defects rather the shallow chondral defects used herein [29]. Briefly, pre-operative sedation with diazepam was provided and a lumbosacral epidural block with lidocaine was placed, followed by induction of general anaesthesia with propofol and maintained by isoflurane. As previously described, a lateral parapatellar mini-arthrotomy was performed on each hind leg [29]. The medial femoral condyle was exposed, and a circular full thickness cartilage defect was made with an 8 mm biopsy punch and subsequent removal of cartilage within the 8 mm defect to create 8 mm × 1–1.25 mm cylindrical large chondral weightbearing defects. To secure the scaffold within the chondral defect, a commercially available osteo-suture screw (Smith&Nephew Twinfix Ti) was used to implant subchondral fixation anchors (cylindrical Ø1.8 mm with a height of 2.8 mm) which were connected to the scaffolds. The Ultrabraid suture supplied with the Twinfix Ti was removed due to its excessive thickness, and rethreaded with a resorbable (PDS II 3–0, Ethicon) or non-resorbable (Prolene 4–0, Ethicon) suture thread (Fig. 1C). Each animal was treated with 2 scaffolds (one per joint) which were fixed using a resorbable ($n = 3$) or a non-resorbable (n = 3) suture thread. The scaffold position was checked, and the surface was palpated to ensure it was flush with the native cartilage tissue [45]. The capsule, subcutis and skin layers were then closed as described earlier [26]. The animals were provided antimicrobial and non-steroidal anti-inflammatory analgesic treatment for 5 days and allowed to mobilise immediately postoperatively.

2.4. Macroscopic evaluation of the large load-bearing articular cartilage defects

At 6 months, euthanasia was carried out with an overdose of sodium pentobarbital administered by I.V. injection. The joints were opened and the defect site and surrounding joint tissues were examined. Photographs of the defect sites were taken and five independent scientists who were blinded to the treatment groups assessed the quality of cartilage repair using a macroscopic evaluation tool (Table 1S) [30,46]. This tool has a maximum score of 8 which represents normal cartilage tissue and rates cartilage repair based on edge integration, smoothness, defect filling and colour of cartilage. Osteochondral segments containing the defect sites surrounded by a margin of approximately 5 mm were subsequently resected and fixed in 10 % formalin for 2–3 days prior to further analysis.

2.5. Micro-computed tomography evaluation of the adjacent subchondral bone

To validate the effectiveness of the suture fixation technique of the scaffold to the adjacent subchondral bone and adjacent cartilage, micro-computed tomography (micro-CT) analysis was performed [47]. All samples were analysed using a Scanco Medical 40 Micro-CT (Bassersdorf, Switzerland) with 70 kVP X-ray source and 112 mA (resolution of ~36 mm). Three-dimensional reconstructions were performed using the Image-J and Bone-J software (public domain software developed by Wayne Rasband in the National Institute of Health, Maryland, USA) and a volume of interest (VOI) was defined within the subchondral bone region of the defect sites. Subchondral bone region was expressed as percentage bone volume over the total volume (% BV/TV). It was calculated by dividing the total volume (TV) with the bone volume (BV) of a defined VOI and made as percentage. The volume of the osteochondral anchor (7.12 mm^3) was subtracted from the TV for non-control samples. Additionally, to assess how the cartilage was regenerating above the implanted osteo-suture anchor, μCT DICOM series were segmented into 3 sections based on their matter density [48]. Regions of interest representing the soft chondral tissue (blue), denser bone tissue (green) and the metallic suture anchor (gold) were processed with the software program Seg3D (version 2.5.1) developed by the NIH Center for Integrative Biomedical Computing (CIBC) with the Scientific Computing and Imaging Institute (SCI) at the University of Utah. Segmented ROI's were then expressed as cross-sectional isosurface renderings to non-invasively asses the tissue explants [49].

2.6. Histological and immunohistochemical evaluation of the large load-bearing articular cartilage defects repair

Specimens were decalcified (Decalcifying Solution-Lite, Sigma-Aldrich, Ireland) prior to histological sectioning. Due to the titanium suture anchor (positioned below the centre of the scaffold) being incompatible with traditional sectioning methods, osteochondral segments containing the defect sites were cut in the near proximity of the anchor to obtain two separate segments representative of the centre of the defect (Fig. 2).

Then, samples were sectioned longitudinally prior to processing using an automated tissue processor (ASP300, Leica, Germany), embedded in paraffin wax blocks and sectioned to a thickness of 10 μm. Sections were stained histologically to assess the quantity and quality of repaired articular cartilage tissue and integration with native tissue. Safranin-O with fast green counterstain was used to assess the presence of sulphated glycosaminoglycan (sGAG) within the repair tissue. Then, to identify the specific type of collagens in the samples, immunohistochemistry was performed for type I and type II collagen. Briefly, antigen retrieval was performed by incubation with Pronase (1μg/mL) (Sigma, Ireland) and Hyaluronidase (10μg/mL) (Sigma, Ireland) with temperature at 37 °C for 30 min. After blocking for nonspecific binding, sections

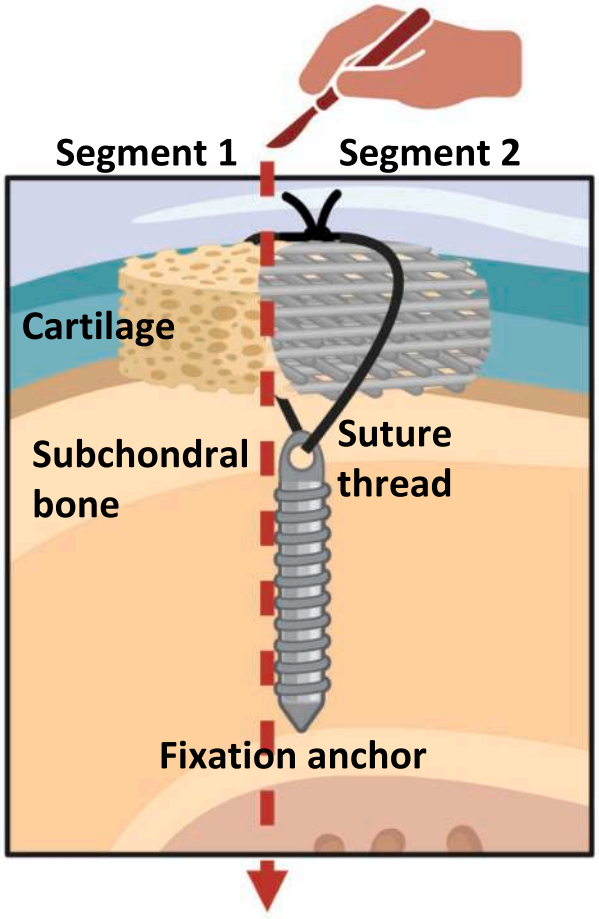

Fig. 2. Illustrative scheme describing the histology preparation of the osteochondral segments containing the defect sites. Due to the titanium suture anchor (positioned below the centre of the scaffold), osteochondral segments were cut in the near proximity of the anchor to obtain two separate segments (1–2) representative of the centre of the defect.

were incubated with primary antibody for type II collagen (Santa Cruz-sc52658 1:100) and type I collagen (Abcam ab90395 1:100) all HRP-conjugated, overnight at 4 °C. Endogenous peroxidase activity was blocked with hydrogen peroxide (Sigma, Ireland) prior to incubation with the anti-mouse IgG secondary antibody (Abcam ab6728 1:500). Sections were then incubated with 3,3′-diaminobenzidine peroxidase substrate (Vector Labs, UK) to visualize positive staining. Finally, sections were developed with DAB peroxidase (Vector Labs, UK) for 10 min. Positive controls (native tissues with primary antibody) and negative controls (native tissues without primary antibody) were included. All sections were successively imaged at several magnifications using a Leica DMIL microscope (Leica Microsystems, Switzerland). Semi-qualitative histological scoring was carried out by five independent scientists under blinded conditions using a modification of the histological scoring system developed by O'Driscoll which has been previously validated for the assessment of articular cartilage repair while also allowing assessment of the subchondral bone (Table 2S) [30,50,51]. The scoring system ranges from 0 (absence of repair) to 28 (normal cartilage tissue) and was used to provide a comprehensive evaluation of repair within the osteochondral defect site using six categories: (I) the nature of cartilage repair tissue (II) structural characteristics, (III) freedom from cellular changes or degradation, (IV) freedom from degradation changes in articular cartilage, (V) reconstitution of subchondral bone and (VI) safranin-O staining.

2.7. Statistical analysis

All statistical analyses were performed using statistics software GraphPad Prism (GraphPad Software 10.2.0, California USA). Results are presented as averages ± standard deviation, and statistical significance was calculated using an ordinary one-way analysis of variance (ANOVA). *P*-values below 0.05 were considered statistically significant where * = $p < 0.05$, ** = $p < 0.01$, *** = $p < 0.001$, and **** = $p < 0.0001$.

3. Results

3.1. Clinical observations after scaffold implantation

During surgery, cell-free biomimetic reinforced CI/II-HyA scaffolds were successfully implanted and secured into the articular cartilage defects in the medial femoral condyles of goats. All scaffolds were easily handled without damage and were seen to fill with blood upon implantation as shown in Fig. 1C. Postoperatively, all animals recovered well and no postoperative complications occurred up to the studies 6-month end point.

3.2. Scaffolds promoted partial formation of new cartilage with most of the full defect area covered in 3 cartilage defects at the early time point of 6 months

Following 6 months implantation, an initial gross visual observation of the opened joints revealed no evidence of inflammation or degenerative changes, construct delamination or migration into the joint cavity. The synovial fluid was biologically normal and clear with a straw colour. Overall, the scaffolds appeared to promote a partial repair of the large chondral defects at the early time point of 6 months (Fig. 3). Macroscopic evaluation of the articular cartilage at the defect site revealed the formation of new cartilage covering most of the full defect area in 3 (Goat 1-Res., Goat 2-Res. and Goat 3-Non-Res.) out of 6 cartilage defects as shown in Fig. 3A. Regardless of whether resorbable or non-resorbable suture threads were used to secure the scaffolds to the defects, scaffolds exhibited signs of smooth hyaline-like articular cartilage tissue formation with satisfactory levels of repair in 3 large chondral defects out of 6. The newly regenerated cartilage appeared to resemble the physiological colour and opaque appearance typical of healthy articular cartilage.

Macroscopic assessment of the defect sites (rating cartilage repair based on edge integration, smoothness of cartilage surface, defect filling and colour of cartilage) performed by 5 independent scientists was analogous to the visual evaluation (Fig. 3B). There were no significant differences in the overall macroscopic scores between groups, although the scaffolds implanted using a non-resorbable suture thread displayed the highest overall macroscopic score of 5.47 ± 1.70 compared to resorbable suture threads 4.53 ± 1.68. When the individual categories were evaluated, scaffolds implanted with non-resorbable suture threads were shown to possess higher individual scores in 3 out of 4 categories. Scaffolds implanted using non-resorbable suture threads had higher scores compared to resorbable in those categories: edge integration (Non-Res: 1.33 ± 0.12; Res: 0.93 ± 0.12); cartilage surface and degree of filling (Non-Res: 1.27 ± 0.55; Res: 0.73 ± 0.46); and smoothness of cartilage surface (Non-Res: 1.27 ± 0.52; Res: 1.20 ± 0.69).

3.3. Scaffolds showed indication to support hyaline-like cartilage formation

Histological analysis revealed indications for the scaffolds to promote hyaline-like cartilage formation at 6 months post-implantation (Fig. 4). Specifically, the scaffolds promoted a partial regeneration of the articular surface with *de novo* deposition of sulphated glycosaminoglycans (sGAG) and type II collagen (collagen II) (key articular cartilage components) in the repaired defect areas. Accordingly to the macroscopic evaluation, 3 scaffolds (Goat 1-Res., Goat 2-Res. and Goat 3-Non-Res.) shown to be well integrated in the defect sites with minor articular cartilage discontinuity between the repaired cartilage and the adjacent tissue. MicroCT segmentation images, which offered the non-destructive characterization of the osteochondral interface in the middle of the defects, confirmed the presence of discernible soft tissue indicative of *de-novo* cartilage formation directly above suture anchors in the defected regions, albeit to varying thicknesses. However, while

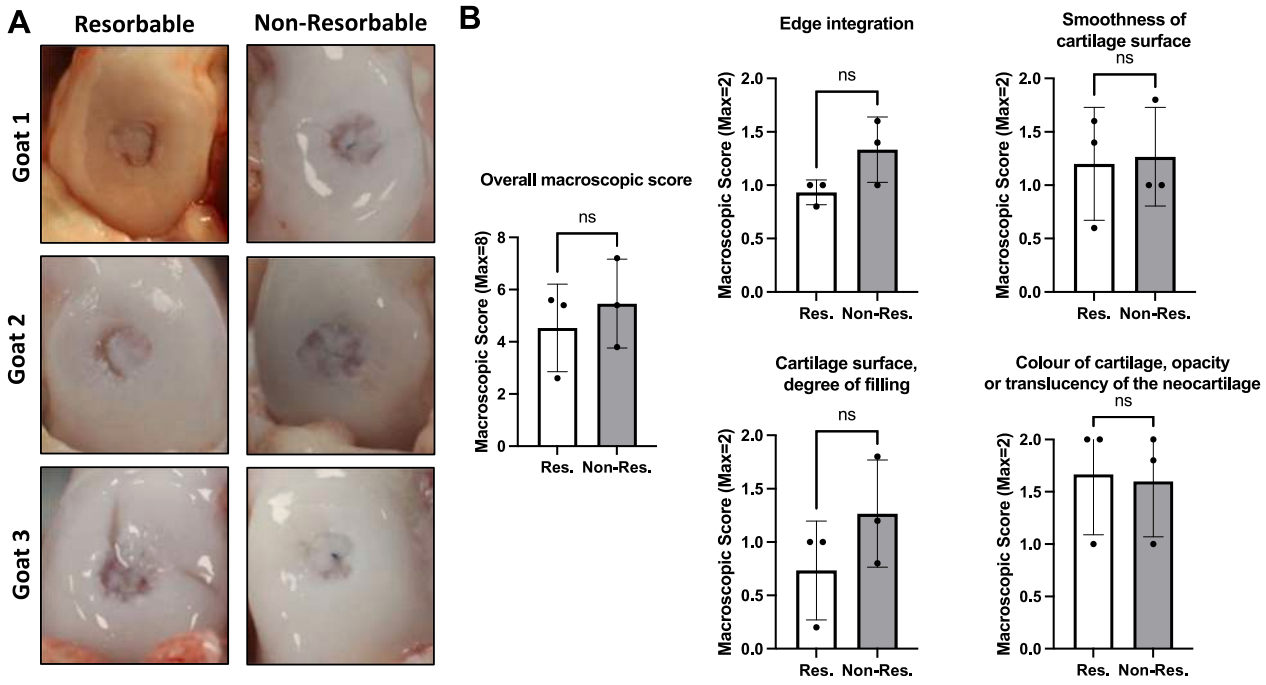

Fig. 3. Scaffolds promoted partial formation of new cartilage with most of the full defect area covered in 3 cartilage defects at 6 months regardless of using resorbable (Res.) or non-resorbable (Non-Res.) suture threads. (A) Macroscopic images (B) and macroscopic scores of large femoral medial condyle defects in goats at 6 months following implantation of the scaffolds using Res. or Non-Res. suture threads ($n = 3$).

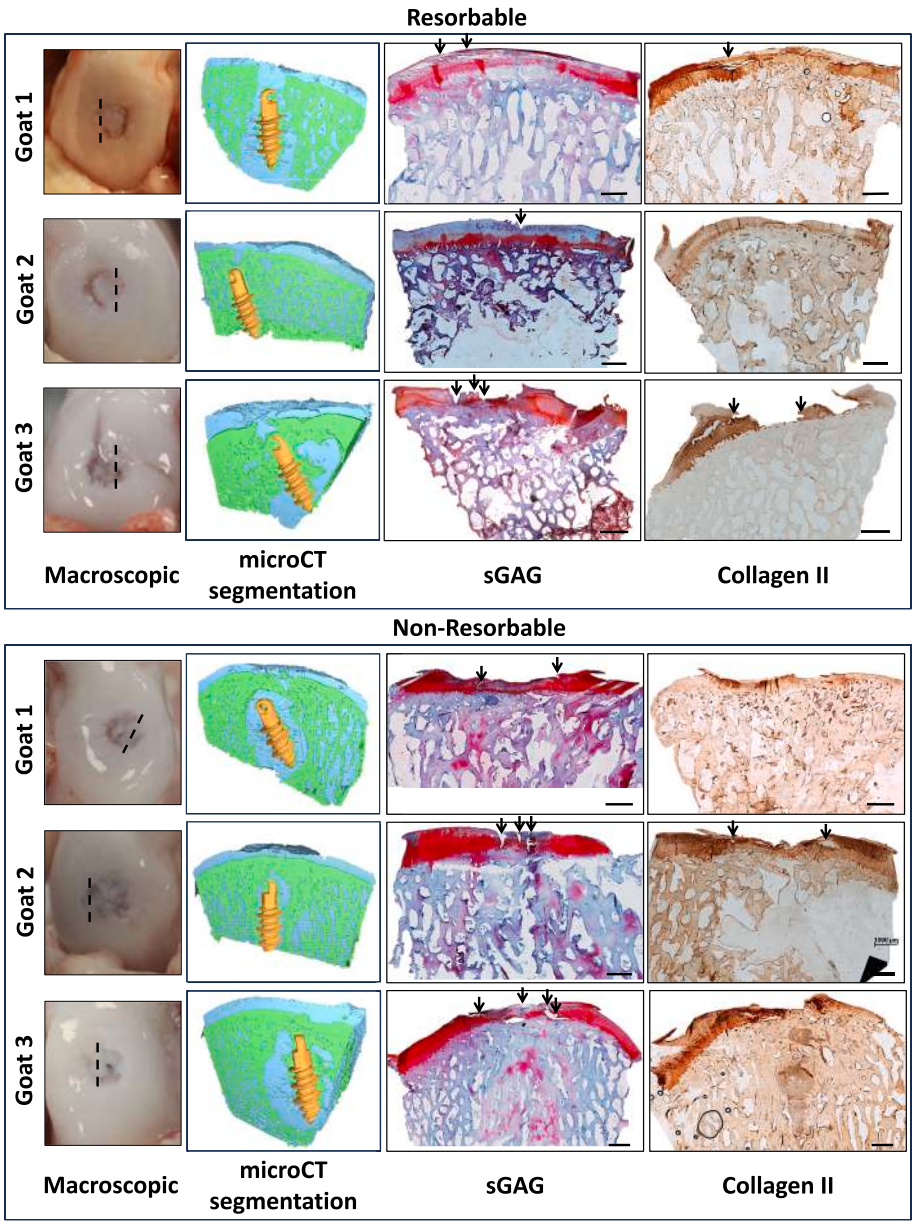

Fig. 4. The scaffolds showed indication to support the partial repair of large defects with the formation of hyaline-like cartilage. On the left, macroscopic images (dashed lines indicate the location of the corresponding stained section) and segmented micro-CT images (representative of the center of the defect) (soft chondral tissue - blue; denser bone tissue – green; and implanted anchor – gold) of large femoral medial condyle defects in goats at 6 months following implantation of the scaffolds using Res. or Non-Res. suture threads ($n = 3$). On the right, representative histological images of the repair tissue stained for Safranin-O (sGAG) and type II collagen (collagen II) (black arrows indicate removed PCL structure). Scale bars indicate 1 mm.

the scaffolds promoted partial repair, some areas of the large defects exhibited small and larger fissures, along with depressed tissue regions on the articular cartilage surface. Additionally, histological images revealed circular voids in the newly formed cartilage, which correspond to the original 3D-printed PCL filaments within the biomimetic reinforced CI/II-HyA scaffolds, as indicated by the arrows in Fig. 4 and asterisks in Fig. 5.

Histological assessment at higher magnification indicated that while the scaffolds facilitated articular cartilage repair, the quality of the regenerated tissue showed some inconsistencies (Fig. 5). A generally hyaline-like morphology was observed, though certain areas exhibited structural irregularities. The repair tissue exhibited mild hypercellularity, and while some cluster formations were present in the deep zone, the overall organization was reasonably comparable to adjacent cartilage. Cells within the cartilage region were found to be sparsely dispersed in the superficial area of the newly formed cartilage with greater abundance in the deeper areas of the tissue with alignment typical of native tissue. Cells appeared to possess a chondrocyte-like morphology with a more pronounced, rounded shape in the deep zone, and elongated shape in the superficial zone parallel to the articular surface.

Furthermore, all scaffolds displayed strong levels of type I collagen in the subchondral bone area, thus, highlighting a hyaline-like cartilage formation with a minimal presence of type I collagen, main bone ECM, in the chondral region (Fig. 6). There were no major differences in type I collagen levels between the groups.

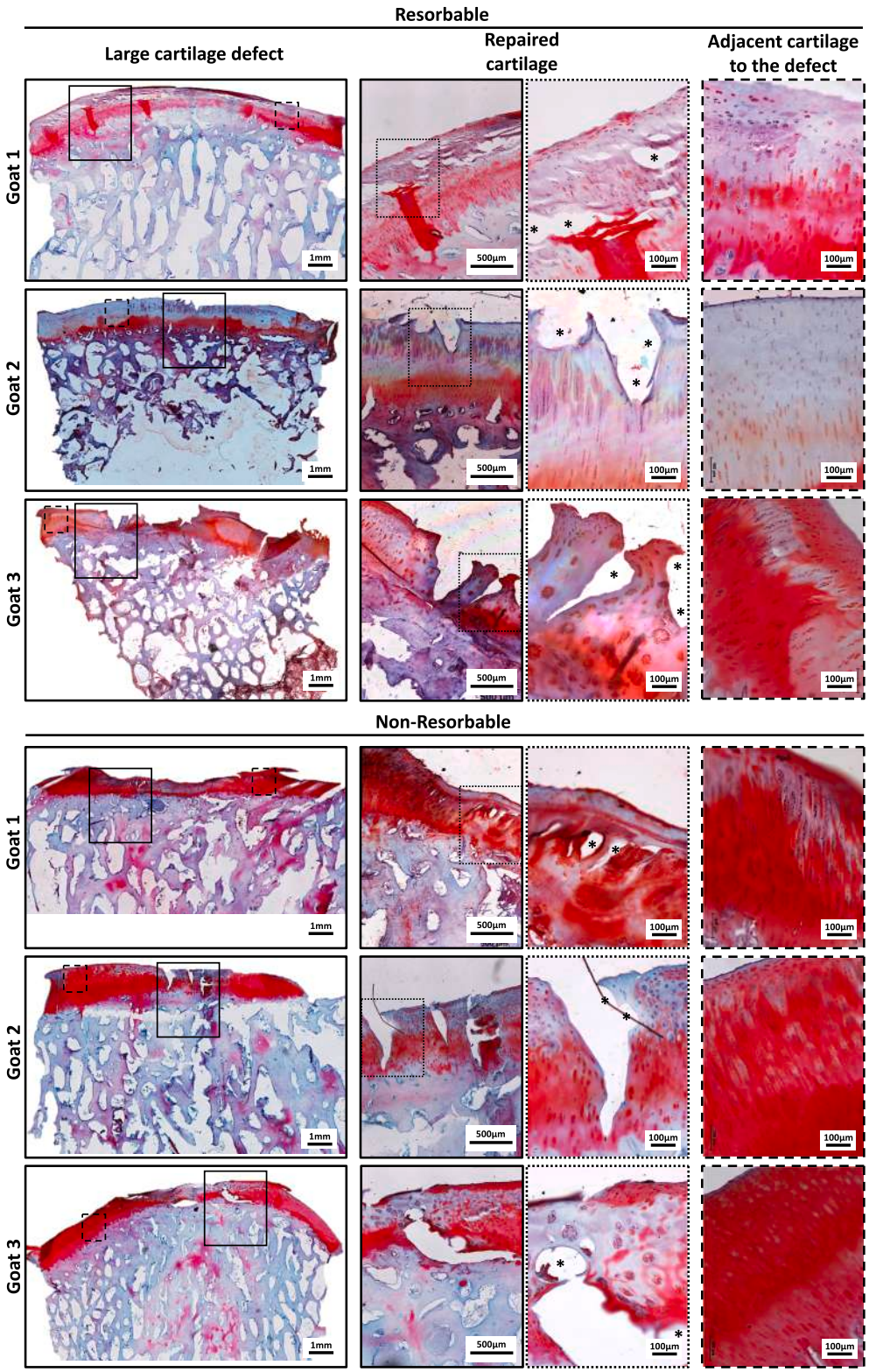

Fig. 5. The scaffolds facilitated direct deposition of new articular cartilage tissue with a hyaline-like morphology and architecture while certain areas exhibited structural irregularities. Representative histological images at different magnifications of adjacent cartilage to the defects and repaired cartilage into defect sites stained for Safranin-O ($n = 3$). Asterisks (*) indicate circular voids in the newly formed cartilage, corresponding to the original 3D-printed PCL filaments within the biomimetic reinforced CI/II-HyA scaffolds.

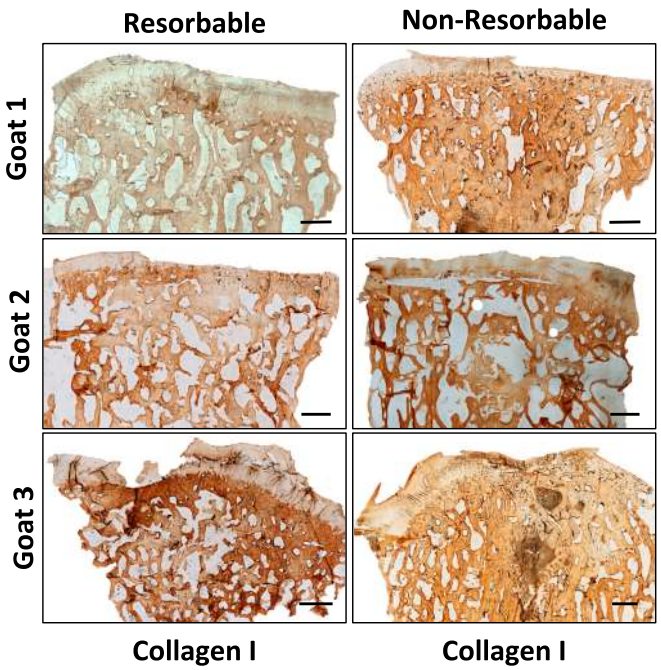

Fig. 6. The scaffolds facilitated a hyaline-like cartilage formation with a minimal presence of type I collagen, main bone ECM, in the chondral region. Representative histological images of repaired tissue stained for type I collagen are presented for each group (n = 3). Scale bars indicate 1 mm.

3.4. The osteo-suture fixation anchors in combination with the non-resorbable suture threads did not cause major damages to the healthy subchondral bone

Following assessment of the large chondral defects, the subchondral region within the defect sites was investigated to assess the efficacy of the fixation technique used to secure the scaffolds. Micro-CT analysis revealed that the osteo-suture fixation anchors, when used in combination with non-resorbable suture threads to secure the scaffolds in large chondral defects, did not cause significant damage to the surrounding healthy subchondral tissue (Fig. 7). Specifically, the BV/TV ratio of scaffolds implanted with non-resorbable suture threads (40.57 %) showed no significant difference compared to the intact native tissue adjacent to the defect sites in the same knee (47.84 %) (Fig. 7B).

Furthermore, micro-CT segmentation analysis, a non-destructive characterization of the osteochondral interface above the implanted suture anchors, indicated that all scaffolds were successfully secured with osteo-suture fixation anchors to the shallow defects throughout the study. However, some formation of uncalcified soft tissue was observed near the subchondral fixation anchors in both groups (Fig. 4). In each case, the osteo-suture anchor remained securely in place, recessed below the chondral defect region.

3.5. Histological scoring revealed that all scaffolds promoted comparable levels of articular cartilage repair

Assessment of articular cartilage repair and of the subchondral bone region was carried out using a validated histological scoring system developed by O'Driscoll [50]. The results revealed that overall all scaffolds promoted comparable levels of articular cartilage repair without affecting the subchondral zone regardless of using resorbable or non-resorbable suture threads (Fig. 8). Although there was no significant difference in the overall histological score between the groups, the scaffolds implanted with a non-resorbable suture thread reported the highest overall score of 20.60 ± 0.72 compared to scaffolds implanted with a resorbable one (17.87 ± 3.58). When the individual categories were evaluated, scaffolds implanted with non-resorbable suture thread displayed higher individual scores in 4 out of 6 categories, with 3 of these being significant compared to scaffolds with a resorbable suture

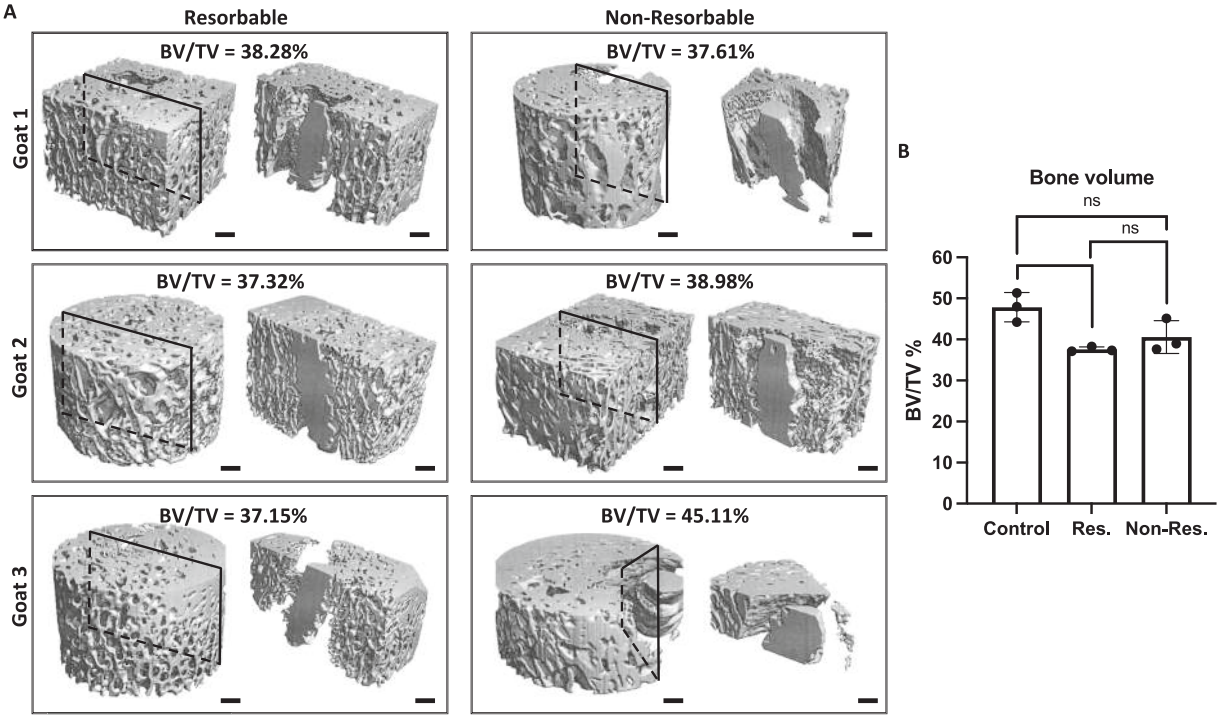

Fig. 7. The osteo-suture fixation anchors in combination with the non-resorbable suture threads did not cause major damages to the healthy subchondral bone. (A) Representative microCT reconstructions of (i) the osteochondral segments containing the defect sites and of (ii) the cross-section (as per projection) of the previous segments. (B) The percentage % of bone volume fraction (BV/TV) was calculated for each sample and compared to the respective positive control representing the native tissue. Scale bars indicate 1 mm.

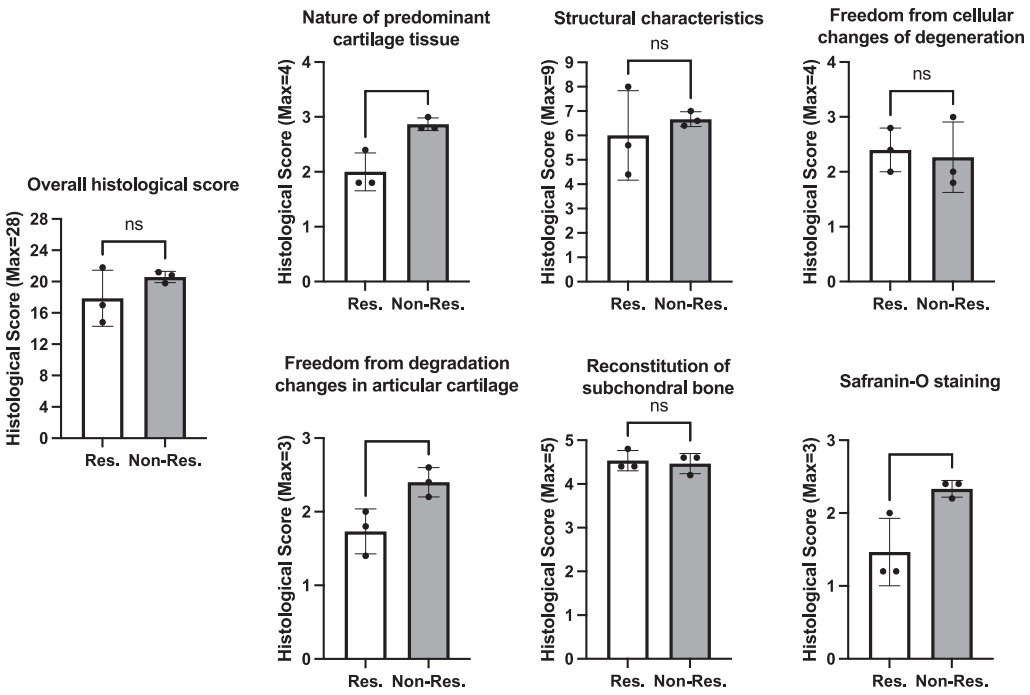

Fig. 8. The scaffolds promoted comparable overall histological scores of articular cartilage repair, with scaffolds implanted with non-resorbable suture threads having higher individual scores in 4 out of 6 categories compared to scaffolds with resorbable suture thread. Total histological scores of large femoral medial condyle defect sites following implantation with scaffolds using resorbable (Res.) or non-resorbable (Non-Res.) suture threads at 6 months ($n = 3$).

thread. Scaffolds implanted using non-resorbable suture threads had higher scores compared to resorbable in the following categories: nature of predominant cartilage tissue (Non-Res: 2.87 ± 0.55; Res: 2.00 ± 0.35); structural characteristic (Non-Res: 6.67 ± 0.46; Res: 6.00 ± 0.64); freedom from degradation changes in articular cartilage (Non-Res: 2.40 ± 0.23; Res: 1.73 ± 0.46); and safranin-O staining (Non-Res: 2.33 ± 0.23; Res: 1.47 ± 0.55).

4. Discussion

The overall aim of this study was to evaluate the capacity of a biomimetic reinforced 3D printed collagen-based scaffold - previously developed *in vitro* - to repair large articular cartilage defects in a load bearing area of the goat medial femoral condyle - in a pilot preclinical study. Additionally, this study aimed to validate the effectiveness of a chondral fixation technique - previously tested *ex-vivo* - to secure the biomimetic reinforced scaffolds to these clinically challenging shallow cartilage defects in the articular joint. This technique uses anchoring of the scaffold to the subchondral bone using a fixation anchor while using sutures to attach the anchor to the scaffold. The study utilised a type I/II collagen-hyaluronic acid (CI/II-HyA) scaffold, mechanically reinforced with a 3D printed PCL framework which has similar mechanical properties to the healthy native tissue and has previously demonstrated strong pro-chondrogenic regenerative capacity *in vitro* [35]. The results from this study demonstrated promise for the scaffolds to repair these large relevant load-bearing articular cartilage defects after 6 months of treatment. Macroscopic and histological evaluation provided indications for the scaffolds to support new hyaline-like cartilage formation partially covering the defect area. Scaffold fixation, which is a common challenge in chondral defect repair, proved to be successful, providing support for future adoption of this approach. Taken together, these findings demonstrate the potential of this biomimetic reinforced scaffold and fixation method to be further investigated pre-clinically with potential to become a viable clinical treatment for large articular cartilage defects.

Initial macroscopic evaluation revealed promising ability for the collagen-based scaffolds to support effective repair with the formation of a new white cartilaginous layer covering most of the defect area in 3 out of 6 cartilage defects at the early 6-month time point. These results align with previous data from our laboratory revealing the capability of a multi-layer collagen-based scaffold for osteochondral repair to heal smaller articular cartilage defects (6 mm diameter) [29,30]. Similarly, our findings confirm that the biomimetic reinforced scaffold enhanced cartilage repair, outperforming empty 6 mm osteochondral defects [29,30]. Furthermore, our results are comparable to other few engineered constructs that have demonstrated some capacity to repair similar-sized articular joint defects [52–54]. However, this study is the first to provide promising evidence that the biomimetic reinforced scaffold can effectively repair larger (8 mm diameter) load-bearing articular cartilage defects, which represent a 75 % greater surface area than those in previous studies [29,30,34]. Unlike previous studies in deeper osteochondral defects, the presented scaffold showed some ability to repair areas covering the cartilage defects alone which presents more advanced challenges than repairing osteochondral tissue [15,55]. These include the avascular nature of cartilage, its limited cellularity, and the difficulty of securing scaffolds in shallow defects [15,55]. The lack of blood supply in cartilage limits the diffusion of nutrients and growth factors essential for repair, whereas osteochondral defects benefit from vascularization and the recruitment of mesenchymal stem cells (MSCs) from the bone marrow. Notably, the level of cartilage repair achieved at 6 months - likely mediated by the recruitment of endogenous progenitor cells - within our biomimetic reinforced scaffold was comparable to biomaterials designed for osteochondral defects, which subsequently exhibited enhanced healing at 12 months [29,34,35,56]. Although further pre-clinical investigation is needed, it is possible that our reinforced biomaterial will continue to support healing at later time points, similar to materials developed for osteochondral repair. Furthermore, the reinforcement of the collagen and hyaluronic acid-based biomaterial with PCL is expected to cause the resultant implant to take up to 2 years to degrade [57–59]. During such time it is expected that the mechanical properties of PCL scaffolds will diminish as the PCL degrades. However, the reduction in PCL's mechanical

properties should be offset by the newly deposited and maturing hyaline-like tissue from within the microporous collagen and hyaluronic acid matrix. The ideal scenario would see no net change in mechanical properties as new tissue is formed. While we do not have data to show this for the current study, future experiments or in-silico modeling might provide new insights into complex transition of load between the degrading biomaterial scaffold and the newly formed tissue over time. Taken together, these findings highlight the potential of the biomimetic reinforced scaffold as a promising "off-the-shelf" biomaterial for the treatment of large chondral defects.

This study further highlighted indications of these reinforced collagen-based scaffolds to promote a hyaline-like cartilage formation, rich in sulphated glycosaminoglycans (sGAG) and type II collagen with minimal type I collagen, a main ECM component of bone and fibrocartilage in the chondral region. The abundant *de-novo* deposition of key articular cartilage ECM components, such as sGAG and type II collagen, indicates the high-quality of the regenerated articular cartilage tissue [60–62]. Clinically, the regeneration of high-quality tissue is crucial to ensure mechanical functionality and the efficacy of the long-term tissue repair [8,9]. However, although the reinforced collagen-based scaffolds promoted high-quality cartilage formation, it is likely that the regenerated tissue has not yet achieved the native mechanical properties of articular cartilage, due to the early time point of analysis. Tissue maturation and remodelling are ongoing, gradual processes, during which the newly formed tissue progressively assumes full load-bearing function [63,64]. The early surface irregularities observed in some specimens may reflect an initial stage of remodelling and are expected to improve over time, supporting the potential for long-term functional restoration. Moreover, histological analysis of defects in this study revealed limited evidence of degenerative changes in the newly regenerated tissues, with chondral layers displaying a hyaline-like morphology, with a mild hypercellularity. While the repair tissue exhibited some cluster formations in the deep zone, the overall organization was reasonably comparable to adjacent cartilage. Previous studies linked treatments resulting in profuse degenerative changes within the repaired articular cartilage to poor tissue repair and frequent revision surgery within 5 years [65–67]. Taken together, these findings provide further support for the potential ability of this scaffold to support long-term cartilage repair in patients.

Furthermore, all scaffolds showed indications of being successfully secured to the shallow defects throughout the study. Unlike osteochondral engineered constructs, which are typically implanted using a press-fit surgical technique, biomaterials confined to cartilage often fail with this technique [13–15]. Previous studies on alternative fixation techniques for chondral biomaterial fixation have often reported promising *in vitro* data that failed to perform well in large animal models [15,37]. Other methods appear also more complicated to use, for instance, fibrin glue scaffold fixation in combination with a periosteal flap covering the defects. These approaches led to relatively poor outcomes with implanted material reported as loose in the joint space, even after 4 weeks of post-surgery joint immobilisation [15,68]. Alternatively, two other studies have investigated the fixation of cartilage implants by converting chondral defects into superficial osteochondral defects (less than half the depth of a typical osteochondral defect) and then using a press-fit technique [15,69]. However, this approach also resulted in a high rate of fixation loss of 20 % and 5 % after 12 weeks implantation, with a higher risk of bone cyst formation in the subchondral bone area [15,69]. Therefore, while further testing is required, the success of our fixation technique is encouraging, considering the current lack of optimal biomaterial fixation strategies for chondral repair [15,37].

This study has also revealed that scaffolds implanted using osteosuture fixation anchors connected to a non-resorbable suture thread did not cause major damages to the original healthy subchondral tissue compared to the resorbable one. Although further investigation is needed, it is possible that the non-resorbable suture provided more mechanical stability to the subchondral fixation anchor, thus resulting in minimised movement with the formation of new repair tissue, later remodelled to strong bone [70]. This result is not surprising given that non-resorbable sutures are often primarily chosen in orthopaedic surgical procedures given the major advantages provided in terms of mechanical stability and support compared to the resorbable ones which offer limited long-term support [42]. Although the resorbable sutures commonly offer advantages with reduced risk of infections and inferior scarring, it appears to be insufficient to surpass the non-resorbable ones for this type of orthopaedic procedure where mechanical stability is paramount [71]. In this context, no histological signs of foreign body reaction or chronic inflammation were observed in the tissue surrounding the non-absorbable sutures at 6 months, suggesting good biocompatibility within the limits of the current observation period. Therefore, the results demonstrate a simple and effective chondral biomaterial fixation technique which can open many avenues of research for application with other engineered cartilage constructs.

5. Conclusion

This study has demonstrated promise for the biomimetic reinforced collagen type I/II-hyaluronic acid (CI/II-HyA) scaffold to repair large clinically challenging articular cartilage defects in a goat medial femoral condyle - a load bearing area in the goat stifle joint - after only 6 months of treatment while also demonstrating the efficacy of a new biomaterial fixation technique. The reinforced CI/II-HyA scaffold in combination with the fixation method has potential to become a viable treatment to repair large chondral defects, presenting an alternative strategy to those available in the clinic.

CRediT authorship contribution statement

Claudio Intini: Writing – review & editing, Writing – original draft, Investigation, Conceptualization. **Michael Joyce:** Writing – review & editing, Investigation, Conceptualization. **Michela Uberti:** Investigation. **Margot C. Labberté:** Investigation. **Giulio Brunetti:** Investigation. **Becky Hackett:** Writing – review & editing. **Tom Hodgkinson:** Writing – review & editing. **John M. O'Byrne:** Conceptualization. **Pieter A.J. Brama:** Writing – review & editing, Investigation, Conceptualization. **Fergal J. O'Brien:** Writing – review & editing, Funding acquisition, Conceptualization.

Declaration of competing interest

Fergal J. O'Brien holds IP with a commercial product of related composition to the collagen-based scaffolds used in this study.

Acknowledgements

This work was financially supported by a European Research Council (ERC) Advanced Grant n°788753 (ReCaP).

References

[1] T. Hodgkinson, D.C. Kelly, C.M. Curtin, F.J. O'Brien, Mechanosignalling in cartilage: an emerging target for the treatment of osteoarthritis, Nat. Rev. Rheumatol. 18 (2022) 67–84.
[2] F. Guilak, R.J. Nims, A. Dicks, C.-L. Wu, I. Meulenbelt, Osteoarthritis as a disease of the cartilage pericellular matrix, Matrix Biol. 71–72 (2018) 40–50.
[3] T. Hodgkinson, I.N. Amado, F.J. O'Brien, O.D. Kennedy, The role of mechanobiology in bone and cartilage model systems in characterizing initiation and progression of osteoarthritis, APL Bioeng 6 (2022).
[4] R.J. Lories, S. Monteagudo, Review article: is Wnt signaling an attractive target for the treatment of osteoarthritis? Rheumatol Ther 7 (2020) 259–270.
[5] V.P. Leifer, J.N. Katz, E. Losina, The burden of OA-health services and economics, Osteoarthr. Cartil. 30 (2022) 10–16.
[6] M. Brittberg, Clinical articular cartilage repair—an up to date review, Ann Jt 3 (2018) 94.

[7] K. Gress, et al., Treatment recommendations for chronic knee osteoarthritis, Best Pract. Res. Clin. Anaesthesiol. 34 (2020) 369–382.
[8] M. Sennett, et al., Long term outcomes of biomaterial-mediated repair of focal cartilage defects in a large animal model, Eur. Cell. Mater. 41 (2021) 40–51.
[9] M. Husen, R.J.H. Custers, M. Hevesi, A.J. Krych, D.B.F. Saris, Size of cartilage defects and the need for repair: a systematic review, Journal of Cartilage & Joint Preservation 2 (2022) 100049.
[10] W. Wei, H. Dai, Articular cartilage and osteochondral tissue engineering techniques: recent advances and challenges, Bioact Mater 6 (2021) 4830–4855.
[11] Y. Wu, et al., Three-dimensional bioprinting of articular cartilage: a systematic review, Cartilage 12 (2021) 76–92.
[12] A. Rahmani Del Bakhshayesh, et al., An overview of various treatment strategies, especially tissue engineering for damaged articular cartilage, Artif Cells Nanomed Biotechnol 48 (2020) 1089–1104.
[13] F. Bothe, et al., Treatment of focal cartilage defects in minipigs with zonal chondrocyte/mesenchymal progenitor cell constructs, Int. J. Mol. Sci. 20 (2019) 653.
[14] A.G. González Vázquez, et al., Systematic comparison of biomaterials-based strategies for osteochondral and chondral repair in large animal models, Adv. Healthc. Mater. 10 (2021) 2100878.
[15] B. Lotz, et al., Preclinical testing of new hydrogel materials for cartilage repair: overcoming fixation issues in a large animal model, Int J Biomater 2021 (2021) 1–14.
[16] A. Rahmani Del Bakhshayesh, et al., An overview of various treatment strategies, especially tissue engineering for damaged articular cartilage, Artif Cells Nanomed Biotechnol 48 (2020) 1089–1104.
[17] A. Trengove, C. Di Bella, A.J. O'Connor, The challenge of cartilage integration: understanding a major barrier to chondral repair, Tissue Eng. Part B Rev. 28 (2022) 114–128.
[18] U. von Mentzer, C. Corciulo, A. Stubelius, Biomaterial integration in the joint: pathological considerations, immunomodulation, and the extracellular matrix, Macromol. Biosci. 22 (2022).
[19] F. Wei, et al., Host response to biomaterials for cartilage tissue engineering: key to remodeling, Front. Bioeng. Biotechnol. 9 (2021).
[20] A. Matsiko, J.P. Gleeson, F.J. O'Brien, Scaffold mean pore size influences mesenchymal stem cell chondrogenic differentiation and matrix deposition, Tissue Eng. Part A 21 (2015) 486–497.
[21] C.M. Murphy, M.G. Haugh, F.J. O'Brien, The effect of mean pore size on cell attachment, proliferation and migration in collagen–glycosaminoglycan scaffolds for bone tissue engineering, Biomaterials 31 (2010) 461–466.
[22] G. Lutzweiler, A. Ndreu Halili, N. Engin Vrana, The overview of porous, bioactive scaffolds as instructive biomaterials for tissue regeneration and their clinical translation, Pharmaceutics 12 (2020) 602.
[23] Y.-Y. Liu, et al., Collagen-based 3D printed poly (glycerol sebacate) composite scaffold with biomimicking mechanical properties for enhanced cartilage defect repair, Int. J. Biol. Macromol. 280 (2024) 135827.
[24] K. Qiao, et al., The advances in nanomedicine for bone and cartilage repair, J Nanobiotechnology 20 (2022) 141.
[25] T.J. Levingstone, A. Matsiko, G.R. Dickson, F.J. O'Brien, J.P. Gleeson, A biomimetic multi-layered collagen-based scaffold for osteochondral repair, Acta Biomater. 10 (2014) 1996–2004.
[26] B.J. Evers, et al., Post-traumatic knee osteoarthritis; the role of inflammation and hemarthrosis on disease progression, Front Med (Lausanne) 9 (2022).
[27] J.E. Dilley, M.A. Bello, N. Roman, T. McKinley, U. Sankar, Post-traumatic osteoarthritis: a review of pathogenic mechanisms and novel targets for mitigation, Bone Rep 18 (2023) 101658.
[28] S. An, et al., A miR-activated hydrogel for the delivery of a pro-chondrogenic microRNA-221 inhibitor as a minimally invasive therapeutic approach for articular cartilage repair, Mater Today Bio 30 (2025) 101382.
[29] T.J. Levingstone, et al., Multi-layered collagen-based scaffolds for osteochondral defect repair in rabbits, Acta Biomater. 32 (2016) 149–160.
[30] T.J. Levingstone, et al., Cell-free multi-layered collagen-based scaffolds demonstrate layer specific regeneration of functional osteochondral tissue in caprine joints, Biomaterials 87 (2016) 69–81.
[31] C. Intini, et al., A highly porous type II collagen containing scaffold for the treatment of cartilage defects enhances MSC chondrogenesis and early cartilaginous matrix deposition, Biomater. Sci. (2022), https://doi.org/10.1039/D1BM01417J.
[32] C. Intini, T. Hodgkinson, S.M. Casey, J.P. Gleeson, F.J. O'Brien, Highly porous type II collagen-containing scaffolds for enhanced cartilage repair with reduced hypertrophic cartilage formation, Bioengineering 9 (2022) 232.
[33] C. Intini, et al., An innovative miR-activated scaffold for the delivery of a miR-221 inhibitor to enhance cartilage defect repair, Adv Ther (Weinh) 6 (2023).
[34] T.J. Levingstone, et al., Evaluation of a co-culture of rapidly isolated chondrocytes and stem cells seeded on tri-layered collagen-based scaffolds in a caprine osteochondral defect model, Biomaterials and Biosystems 8 (2022) 100066.
[35] M. Joyce, et al., Development of a 3D-printed bioabsorbable composite scaffold with mechanical properties suitable for treating large, load-bearingarticular cartilage defects, Eur. Cell. Mater. 45 (2023) 158–172.
[36] M. Joyce, et al., Gene activated reinforced scaffolds for SOX9 delivery to enhance repair of large load bearing articular cartilage defects, Eur. Cell. Mater. 47 (2024) 91–108.
[37] I.A.D. Mancini, et al., Fixation of hydrogel constructs for cartilage repair in the equine model: a challenging issue, Tissue Eng. Part C Methods 23 (2017) 804–814.
[38] A. Vahdati, D.R. Wagner, Implant size and mechanical properties influence the failure of the adhesive bond between cartilage implants and native tissue in a finite element analysis, J. Biomech. 46 (2013) 1554–1560.
[39] B. Lotz, et al., Preclinical testing of new hydrogel materials for cartilage repair: overcoming fixation issues in a large animal model, Int J Biomater 2021 (2021) 1–14.
[40] S. Knecht, et al., Mechanical testing of fixation techniques for scaffold-based tissue-engineered grafts, J. Biomed. Mater. Res. B Appl. Biomater. 83B (2007) 50–57.
[41] M. Drobnič, D. Radosavljevič, D. Ravnik, V. Pavlovčič, M. Hribernik, Comparison of four techniques for the fixation of a collagen scaffold in the human cadaveric knee, Osteoarthr. Cartil. 14 (2006) 337–344.
[42] P. D'Cunha, et al., Absorbable sutures: chronicles and applications, International Surgery Journal 9 (2022) 1383.
[43] M.G. Haugh, C.M. Murphy, F.J. O'Brien, Novel freeze-drying methods to produce a range of collagen–glycosaminoglycan scaffolds with tailored mean pore sizes, Tissue Eng. Part C Methods 16 (2010) 887–894.
[44] M.G. Haugh, C.M. Murphy, R.C. McKiernan, C. Altenbuchner, F.J. O'Brien, Crosslinking and mechanical properties significantly influence cell attachment, proliferation, and migration within collagen glycosaminoglycan scaffolds, Tissue Eng. Part A 17 (2011) 1201–1208.
[45] J.L. Koh, K. Wirsing, E. Lautenschlager, L.-O. Zhang, The effect of graft height mismatch on contact pressure following osteochondral grafting, Am. J. Sports Med. 32 (2004) 317–320.
[46] A.M.J. Getgood, et al., Evaluation of early-stage osteochondral defect repair using a biphasic scaffold based on a collagen–glycosaminoglycan biopolymer in a caprine model, Knee 19 (2012) 422–430.
[47] E. Andrés Sastre, et al., A new semi-orthotopic bone defect model for cell and biomaterial testing in regenerative medicine, Biomaterials 279 (2021) 121187.
[48] T. Kamio, M. Suzuki, R. Asaumi, T. Kawai, DICOM segmentation and STL creation for 3D printing: a process and software package comparison for osseous anatomy, 3D Print Med 6 (2020) 17.
[49] Y. Nagai, Y. Ohtake, H. Suzuki, SegMo: CT volume segmentation using a multi-level Morse complex, Comput. Aided Des. 107 (2019) 23–36.
[50] S.W. O'Driscoll, F.W. Keeley, R.B. Salter, The chondrogenic potential of free autogenous periosteal grafts for biological resurfacing of major full-thickness defects in joint surfaces under the influence of continuous passive motion. An experimental investigation in the rabbit, J. Bone Joint Surg. Am. 68 (1986) 1017–1035.
[51] M. Rutgers, M.J.P. van Pelt, W.J.A. Dhert, L.B. Creemers, D.B.F. Saris, Evaluation of histological scoring systems for tissue-engineered, repaired and osteoarthritic cartilage, Osteoarthr. Cartil. 18 (2010) 12–23.
[52] M. Jung, S. Breusch, W. Daecke, T. Gotterbarm, The effect of defect localization on spontaneous repair of osteochondral defects in a Göttingen minipig model: a retrospective analysis of the medial patellar groove versus the medial femoral condyle, Lab. Anim 43 (2009) 191–197.
[53] W. Brehm, et al., Repair of superficial osteochondral defects with an autologous scaffold-free cartilage construct in a caprine model: implantation method and short-term results, Osteoarthr. Cartil. 14 (2006) 1214–1226.
[54] A.I. Vasara, et al., Subchondral bone reaction associated with chondral defect and attempted cartilage repair in goats, Calcif. Tissue Int. 74 (2003) 107–114.
[55] C. Lesage, et al., Material-assisted strategies for osteochondral defect repair, Adv. Sci. 9 (2022).
[56] E. Kon, et al., Reconstruction of large osteochondral defects using a hemicondylar aragonite-based implant in a caprine model, Arthroscopy: The Journal of Arthroscopic & Related Surgery 36 (2020) 1884–1894.
[57] M. Bartnikowski, T.R. Dargaville, S. Ivanovski, D.W. Hutmacher, Degradation mechanisms of polycaprolactone in the context of chemistry, geometry and environment, Prog. Polym. Sci. 96 (2019) 1–20.
[58] J.R. Dias, A. Sousa, A. Augusto, P.J. Bártolo, P.L. Granja, Electrospun polycaprolactone (PCL) degradation: an in vitro and in vivo study, Polymers (Basel) 14 (2022) 3397.
[59] M.V. Deshpande, A. Girase, M.W. King, Degradation of poly(ε-caprolactone) resorbable multifilament yarn under physiological conditions, Polymers (Basel) 15 (2023) 3819.
[60] L. Alcaide-Ruggiero, V. Molina-Hernández, M.M. Granados, J.M. Domínguez, Main and minor types of collagens in the articular cartilage: the role of collagens in repair tissue evaluation in chondral defects, Int. J. Mol. Sci. 22 (2021) 13329.
[61] A.R. Armiento, M. Alini, M.J. Stoddart, Articular fibrocartilage - why does hyaline cartilage fail to repair? Adv. Drug Deliv. Rev. 146 (2019) 289–305.
[62] D.C. Browe, et al., Promoting endogenous articular cartilage regeneration using extracellular matrix scaffolds, Mater Today Bio 16 (2022) 100343.
[63] T.J. Levingstone, et al., Evaluation of a co-culture of rapidly isolated chondrocytes and stem cells seeded on tri-layered collagen-based scaffolds in a caprine osteochondral defect model, Biomaterials and Biosystems 8 (2022) 100066.
[64] T.J. Levingstone, et al., Cell-free multi-layered collagen-based scaffolds demonstrate layer specific regeneration of functional osteochondral tissue in caprine joints, Biomaterials 87 (2016) 69–81.
[65] S.M. Gillinov, et al., Incidence, timing, and risk factors for 5-year revision surgery after autologous chondrocyte implantation in 533 patients, Am. J. Sports Med. 50 (2022) 2893–2899.
[66] E.S. Mameri, et al., Revision lateral femoral condyle osteochondral allograft transplantation with the snowman technique after failed previous oblong osteochondral allograft, Arthrosc. Tech. 12 (2023) e363–e370.
[67] L. Goebel, D. Kohn, H. Madry, Biological reconstruction of the osteochondral unit after failed focal resurfacing of a chondral defect in the knee, Am. J. Sports Med. 44 (2016) 2911–2916.

[68] W. Brehm, et al., Repair of superficial osteochondral defects with an autologous scaffold-free cartilage construct in a caprine model: implantation method and short-term results, Osteoarthr. Cartil. 14 (2006) 1214–1226.
[69] P. Mainil-Varlet, et al., Articular cartilage repair using a tissue-engineered cartilage-like implant: an animal study, Osteoarthr. Cartil. 9 (2001) S6–S15.
[70] T.H. Shalev, G.M. Kurtzman, A.H. Shalev, D.K. Johnson, M.E.M. Kersten, Continuous periosteal strapping sutures for stabilization of osseous grafts with resorbable membranes for buccal ridge augmentation: a technique report, Journal of Oral Implantology 43 (2017) 283–290.
[71] E. Pacer, D.W. Griffin, A.B. Anderson, S.M. Tintle, B.K. Potter, Suture and needle characteristics in orthopaedic surgery, JBJS Rev 8 (2020) e19.00133.